

# Role of the charge, carbon chain length, and content of surfactant on the skin penetration of meloxicam-loaded liposomes

Sureewan Duangjit<sup>1,2</sup>  
Boonnada  
Pamornpathomkul<sup>1</sup>  
Praneet Opanasopit<sup>1</sup>  
Theerasak Rojanarata<sup>1</sup>  
Yasuko Obata<sup>2</sup>  
Kozo Takayama<sup>2</sup>  
Tanasait Ngawhirunpat<sup>1</sup>

<sup>1</sup>Faculty of Pharmacy, Silpakorn University, Nakhon Pathom, Thailand;

<sup>2</sup>Department of Pharmaceutics, Hoshi University, Shinagawa-ku, Tokyo, Japan



Correspondence: Tanasait Ngawhirunpat  
Faculty of Pharmacy, Silpakorn University,  
Sanamchandra Palace Campus,  
6 Ratchamankana Road, Muang,  
Nakhon Pathom 73000, Thailand  
Tel +66 34 255 800  
Email [tanasait@su.ac.th](mailto:tanasait@su.ac.th)

**Abstract:** The objective of this study was to investigate the influence of surfactant charge, surfactant carbon chain length, and surfactant content on the physicochemical characteristics (ie, vesicle size, zeta potential, elasticity, and entrapment efficiency), morphology, stability, and in vitro skin permeability of meloxicam (MX)-loaded liposome. Moreover, the mechanism for the liposome-enhanced skin permeation of MX was determined by Fourier transform infrared spectroscopy and differential scanning calorimetry. The model formulation used in this study was obtained using a response surface method incorporating multivariate spline interpolation (RSM-S). Liposome formulations with varying surfactant charge (anionic, neutral, and cationic), surfactant carbon chain length (C4, C12, and C16), and surfactant content (10%, 20%, and 29%) were prepared. The formulation comprising 29% cationic surfactant with a C16 chain length was found to be the optimal liposome for the transdermal delivery of MX. The skin permeation flux of the optimal formulation was 2.69-fold higher than that of a conventional liposome formulation. Our study revealed that surfactants affected the physicochemical characteristics, stability, and skin permeability of MX-loaded liposomes. These findings provide important fundamental information for the development of liposomes as transdermal drug delivery systems.

**Keywords:** optimal liposome, optimization, transdermal drug delivery, surfactant charge, surfactant carbon chain length, surfactant content

## Introduction

Meloxicam (MX) is an effective nonsteroidal anti-inflammatory drug for reducing pain and inflammatory symptoms.<sup>1-3</sup> Long-term therapy with high doses of MX can lead to gastrointestinal side effects such as upset stomach, indigestion, ulceration, and bleeding.<sup>4</sup> Moreover, the high content of organic solvent in the MX formulation<sup>5,6</sup> limits its safety for skin delivery. Therefore, the development of MX as a transdermal drug delivery (TDD) candidate presents many challenges.

Since the first report that lipid vesicles incorporating sodium cholate as a surfactant could penetrate deep into intact skin to deliver drugs,<sup>7</sup> the use of surfactants in liposome formulations as penetration enhancers for the TDD of various drugs has attracted considerable interest. Numerous formulations have incorporated various types of surfactants in liposome bilayers. Although the use of cationic surfactants in liposomes has been reported to enhance the skin delivery of several drugs,<sup>8-11</sup> anionic surfactants in liposomes are also effective in improving skin delivery.<sup>12-14</sup> The influence of surfactants on the effectiveness of liposomes for skin delivery remains a much-debated question. Herein, liposome delivery systems must be designed and evaluated on a case-by-case basis because surfactants exhibit a diverse variety of hydrophilic head groups and

lipophilic carbon chain lengths. Thus, comparisons of previous research on liposome formulations composed of various surfactant types are difficult to make. Furthermore, the skin models and conditions used to evaluate the surfactants also vary widely. To date, no proper method for estimating the effects of individual surfactant factor (eg, charge, carbon chain length, and content) on the intrinsic properties of liposomes has yet been established. As a result, a rational approach for designing liposome formulations containing surfactants for skin delivery has not yet been fully described.

In this study, three types of liposome carriers neutral conventional liposomes (N-CLP), anionic transfersomes (A-TFS), and cationic transfersomes (C-TFS) were prepared as skin delivery carriers of MX. The vesicle composition ratio was obtained from a two-factor spherical second-order composite experimental design. The influences of the charge, carbon chain length, and content of surfactant on the physicochemical characteristics (ie, vesicle size, zeta potential, elasticity, and entrapment efficiency [EE]), morphology, *in vitro* skin permeation, and stability of the liposome formulation were evaluated. The possible mechanisms for the surfactant-enhanced skin permeability of MX-loaded liposomes were also investigated.

## Materials and methods

### Materials

Phosphatidylcholine (PC) from soybean (90%) was generously supplied by Lipoid GmbH (Ludwigshafen, Germany). Cholesterol (Chol) was purchased from Wako Pure Chemical Industries (Osaka, Japan). Butylpyridinium chloride, laurylpyridinium chloride, and cetylpyridinium chloride (CPC) were purchased from MP Biomedicals (Santa Ana, California, USA). Sodium hexadecyl sulfate (SHS) was purchased from Tokyo Chemical Industry Co., Ltd (Tokyo, Japan). MX was supplied by Sigma-Aldrich Production GmbH, (Buchs, Switzerland). All other chemicals used were of reagent grade and were purchased from Wako Pure Chemical Industries.

### Optimization of liposome formulation

The liposome formulation was composed of a constant concentration of PC (10 mM) as the vesicle-forming bilayer, and varying concentrations of Chol and surfactant as a membrane stabilizer and penetration enhancer, respectively. The concentrations of Chol and surfactant varied from 0%–90% molar ratios of PC to determine the optimal Chol and surfactant concentrations in the liposome formulation. Moreover, the MX concentration varied from 0%–20% weight/weight (w/w) of PC to maximize the drug loading in the liposome formulation.

The maximum drug-loading capacity and molar turbidity of the liposome formulations were the selection criteria used to determine the optimal vesicle composition of the liposome formulation. Liposomes and transfersomes were prepared according to formulations obtained from a two-factor spherical-order composite experimental design.<sup>15</sup> The optimal formulation was defined as the maximum flux value of MX permeating the skin for 12 hours. The dataNESIA program (v 3.2; Azbil Corporation, Tokyo, Japan) was used to draw the response surfaces for each variable and predict the response variables (skin permeation flux) of the optimal formulations. Once the optimal formulation estimated with response surface method incorporating multivariate spline interpolation (RSM-S) was obtained, its reliability was evaluated using bootstrap resampling, which has been fully described previously.<sup>16,17</sup> The vesicle composition ratio of the optimal formulation was used as the model composition ratio for further formulations.

### Preparation of MX-loaded liposomes and MX suspensions

Three types of liposome carriers (N-CLP, A-TFS, and C-TFS) were prepared according to the vesicle composition ratio obtained from our optimization study. The chemical structures of the vesicle compositions are displayed in Figure 1. As shown in Table 1, vesicle formulations were prepared by the sonication method.<sup>18</sup> Briefly, lipid mixtures of PC, Chol, surfactant, and MX were dissolved in chloroform/methanol (2:1 volume/volume [v/v] ratio), and the solvent was evaporated under a nitrogen gas stream. The lipid film was dried in a desiccator for 6 hours to remove the remaining solvent. The dried lipid film was hydrated with acetate buffer solution (pH 5.5). Vesicles were subsequently sonicated for 30 minutes using a bath-type sonicator (5510J-DTH; Branson Ultrasonics, Danbury, CT, USA), then sonicated a second time in an ice bath using a probe sonicator (Vibra-Cell™; Sonics and Materials, Inc., Newtown, CT, USA) for 30 minutes. The excess lipid composition was removed by centrifugation at 4°C and 15,000 rpm for 15 minutes, and the supernatant was collected. All formulations were freshly prepared or stored in air-tight containers at 4°C prior to further studies.

The MX suspension was prepared by adding MX to acetate buffer solution (pH 5.5) at a concentration ten times higher than the solubility of MX and stirring for 48 hours to ensure constant thermodynamic activity throughout the course of the permeation experiment. The concentration of MX in the suspension was determined, and the MX suspension was used as a control in the skin permeation experiment.

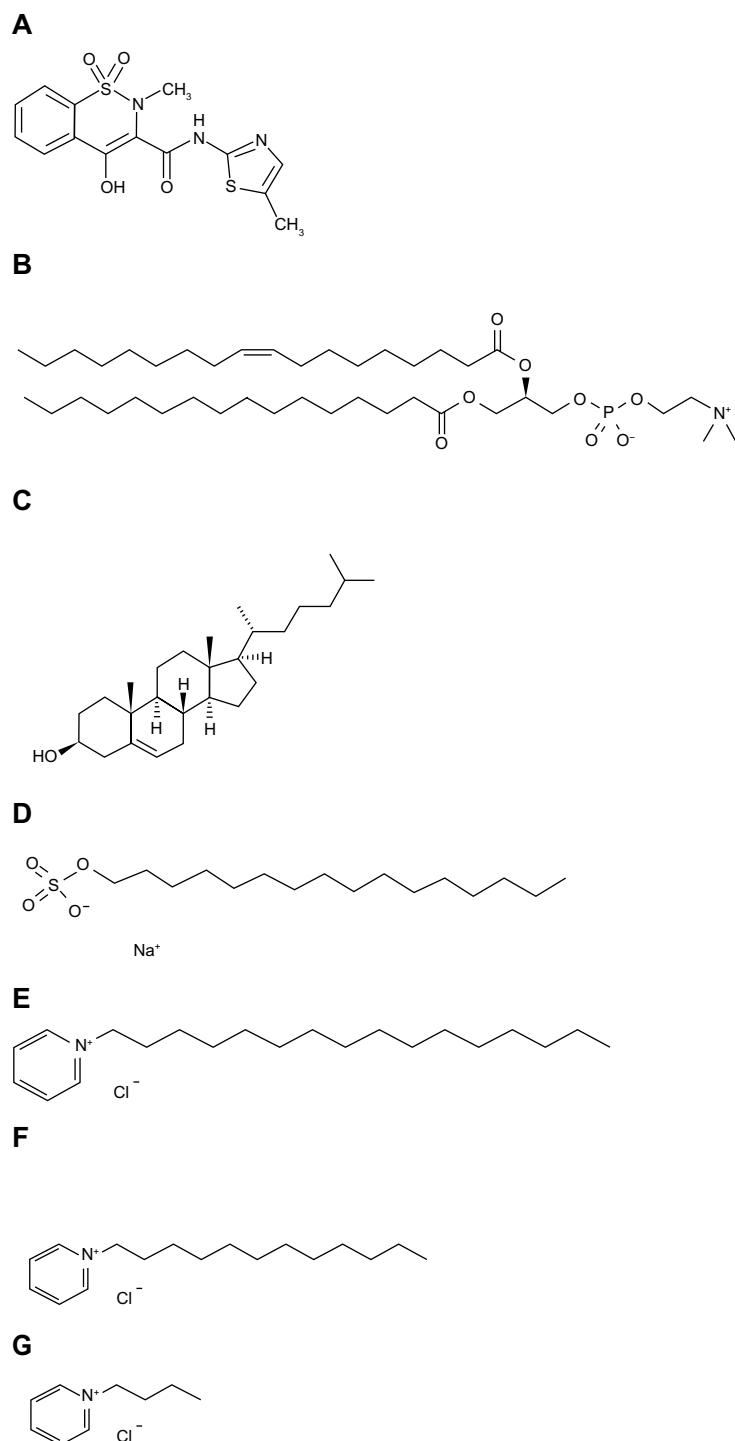


**Figure 1** The chemical structures of the vesicle compositions.

**Notes:** (A) Meloxicam; (B) phosphatidylcholine; (C) cholesterol; (D) sodium hexadecyl sulfate; (E) cetylpyridinium chloride; (F) laurylpyridinium chloride; (G) butylpyridinium chloride.

## Vesicle size and zeta potential investigation

The average vesicle size (nm) and zeta potential (mV) of the vesicle formulations were measured by photon correlation spectroscopy (PCS) (Zetasizer Nano series; Malvern

Instruments, Malvern, UK). Twenty microliters of each vesicle formulation were diluted with 1,480  $\mu\text{L}$  of deionized water. All measurements were performed at room temperature, at least three independent samples were collected, and the vesicle size and zeta potential were measured in triplicate.

**Table 1** Liposome and transfersome formulation

Surfactant factor	Code	Lipid component (%w/v)							Acetate buffer (mL)
		MX	PC	Chol	C4	C12	C16	A16	
Charge	N-CLP	0.07	0.77	0.04	–	–	–	–	100
	C-TFS	0.07	0.77	0.04	–	–	0.10	–	100
	A-TFS	0.07	0.77	0.04	–	–	–	0.10	100
Carbon chain length	C4	0.07	0.77	0.04	0.05	–	–	–	100
	C12	0.07	0.77	0.04	–	0.08	–	–	100
	C16	0.07	0.77	0.04	–	–	0.10	–	100
Content	0% CPC	0.07	0.77	0.04	–	–	–	–	100
	10% CPC	0.07	0.77	0.04	–	–	0.04	–	100
	20% CPC	0.07	0.77	0.04	–	–	0.07	–	100
	29% CPC	0.07	0.77	0.04	–	–	0.10	–	100

**Note:** The concentration of PC in the formulation was fixed at 10 mM. C4, cationic surfactant with 4 carbons; C12, cationic surfactant with 12 carbons; C16, cationic surfactant with 16 carbons; A16, anionic surfactant with 16 carbons.

**Abbreviations:** A-TFS, anionic transfersomes; Chol, cholesterol; CPC, cetylpyridinium chloride; C-TFS, cationic transfersomes; MX, meloxicam; N-CLP, neutral conventional liposome; PC, phosphatidylcholine.

The morphology of the liposomes was characterized using freeze-fractured transmission electron microscopy. A drop of sample solution placed on a small copper block was rapidly frozen in nitrogen slush, which was freshly prepared immediately prior to use by decompression in a vacuum chamber.<sup>19</sup> The quenched sample was fractured in a freeze-fracture apparatus (JFD-9010; JEOL, Tokyo, Japan). The fractured surface was rotary-shadowed with platinum-carbon at an angle of 10°, and the shadowed surface was coated with carbon. The freeze-fractured replica obtained was washed with chloroform/methanol (4:1 v/v ratio) and observed with a JEM-1400 transmission electron microscope (JEOL) equipped with a digital charge-coupled device camera (ES500W Erlangshen; Gatan, Inc., Pleasanton, CA, USA).

## Elasticity evaluation

The elasticity value of the lipid bilayer of the vesicles was directly proportional to  $J_{\text{Flux}} \times (r_v/r_p)^2$ :

$$\text{Elasticity value (mg} \cdot \text{sec}^{-1} \cdot \text{cm}^{-2}) = J_{\text{Flux}} \times \left( \frac{r_v}{r_p} \right)^2, \quad (1)$$

where  $J_{\text{Flux}}$  is the rate of penetration through a permeable barrier ( $\text{mg} \cdot \text{sec}^{-1} \cdot \text{cm}^{-2}$ );  $r_v$  is the size of the vesicles after extrusion (nm); and  $r_p$  is the pore size of the barrier (nm).<sup>20</sup> To measure  $J_{\text{Flux}}$ , the vesicles were extruded through a polycarbonate membrane (Nuclepore; GE Healthcare Life Sciences, Buckinghamshire, UK) with a pore diameter of 50 nm ( $r_p$ ) at a pressure of 0.5 MPa. Five minutes after extrusion, the extrudate was weighed ( $J_{\text{Flux}}$ ) and the average vesicle diameter ( $r_v$ ) was measured by PCS.

## Drug EE (%EE)

The excess lipid composition was removed from the MX-loaded liposome formulation by centrifugation. The concentration of MX in the formulation was determined by high-performance liquid chromatography (HPLC) analysis after disruption of the vesicles with Triton® X-100 (Amresco; Solon, Ohio, USA) (0.1% w/v) at a 1:1 volume ratio and diluted with phosphate-buffered saline (pH 7.4). The vesicle/Triton® X-100 solution was centrifuged at 10,000 rpm at 4°C for 10 minutes. The supernatant was filtered with a 0.45 µm nylon syringe filter. The EEs of the MX loaded in the formulations were calculated according to the following equation:

$$\%EE = \left( \frac{C_L}{C_i} \right) \times 100, \quad (2)$$

where  $C_L$  is the concentration of MX loaded in the formulation, as described above, and  $C_i$  is the initial concentration of MX added to the formulation.

## In vitro skin permeation studies

The shed skin of *Naja kaouthia* was used as a permeation model membrane because a previous study reported that it exhibits similar permeability to human skin.<sup>21</sup> It was donated by the Queen Saovabha Memorial Institute, Thai Red Cross Society, Bangkok, Thailand. Whole snake skins were obtained immediately after shedding from five to seven different snakes. Each snake skin was divided into 10–12 pieces. The thickness of the shed snake skins was approximately 0.02–0.03 mm. They were stored at –10°C

prior to use. After thawing, the skin was cut and then immediately placed on a side-by-side diffusion cell with an available diffusion area of 0.95 cm<sup>2</sup>. The shed snake skin was mounted between the diffusion cells connected with a 32°C ± 1°C control temperature jacket. The stratum corneum (SC) side of the skin faced the donor chamber, which was filled with 3 mL of MX-loaded vesicle formulation and/or MX suspension. The receiving chamber was also filled with 3 mL of 0.1 M phosphate-buffered solution (pH 7.4) and stirred with a star-head magnetic stir bar driven by a synchronous motor. The sink condition in the receiving medium was determined in this study. At appropriate intervals of 2, 4, 6, 8, 10, and 12 hours, 0.5 mL aliquots of the receiving medium were withdrawn and immediately replaced with an equal volume of fresh buffer solution. The concentration of drug in the receiving medium was analyzed by HPLC, and the cumulative amount (µg/cm<sup>2</sup>) was plotted against time. The steady-state flux value was determined as the slope of the linear portion of the plot.

### Stability evaluation

The MX-loaded vesicle formulations were prepared (at least 400 samples) and kept in the glass bottles at 4°C for 200 bottles and 25°C for 200 bottles. The physicochemical stability of the MX-loaded vesicle formulations, such as vesicle size and zeta potential, were evaluated by PCS. The MX remaining in the formulation was determined by HPLC at days 1, 7, 15, 30, and 120. The results of the physicochemical characterization immediately after preparation (at day 1) were used as a control, and the MX entrapped in the formulation at day 1 was also normalized to 100%.

### HPLC analysis

The MX concentration was analyzed by HPLC. All samples were stored at 4°C until analysis. The HPLC system comprised a SIL-20A autosampler, an LC-20AT liquid chromatograph, and an SPD-20AUV detector (Shimadzu Corporation, Kyoto, Japan). The analytical column was a YMC-Pack ODS-A (150×4.6 mm inner diameter, S-5; YMC Co., Ltd, Kyoto, Japan), and the mobile phase was composed of acetate buffer solution (pH 4.6)/methanol (50:50, v/v). The flow rate was set at 0.8 mL/minute, and the wavelength used was 272 nm. The calibration curve for MX was in the range of 1–50 µg/mL with a correlation coefficient of 0.999. The percent recovery ranged from 99.85%–100.30%, and the relative standard deviations for both the intraday and inter-day measurements were less than 2%.

## The mechanisms of liposomes on skin permeation

Following the skin permeation experiment, the shed snake skin was washed with water, blotted dry, and stored in a desiccator. The spectrum of the skin sample was recorded in the range of 500–4,000 cm<sup>-1</sup> using Fourier transform infrared spectroscopy (FTIR) (Nicolet 4700 spectrophotometer; Thermo Fisher Scientific, Waltham, MA, USA). The FTIR spectra of the skin treated with the MX suspension was also recorded and used as a control. Thermal analysis of the shed snake skin following the permeation experiment, prepared using the same method used for the FTIR analysis, was performed with differential scanning calorimetry ([DSC] Pyris Sapphire DSC; PerkinElmer, Waltham, MA, USA). The skin sample (2 mg) was weighed into an aluminum seal pan and was heated from 0°C to 300°C at a heating rate of 10°C/minute. All DSC measurements were collected under a nitrogen atmosphere with a flow rate of 30 mL/minute. The DSC thermograms of the skin treated with the MX suspension was also recorded and used as a control.

The existence of intact vesicles in the release medium after the in vitro skin permeation study was characterized by PCS. Moreover, the release medium following the in vitro skin permeation study was also characterized for PC using a Phosphatidylcholine Assay Kit (Cat No.83377; Abcam®, Cambridge, UK), and the compositions of the intact liposomes or non-intact vesicles in the release medium were determined.

### Data analysis

The data are reported as the means ± standard error (n=3–6), and statistical analysis of the data was carried out using one-way analysis of variance followed by the Student's *t*-test. A *P*-value of less than 0.05 was considered to be statistically significant.

## Results and discussion

### Optimal liposome formulation

Based on its maximum drug-loading capacity and molar turbidity, the vesicle formulation composed of over 40% Chol and surfactant likely reassembled to a mixed micelle structure. Liposomes and mixed micelle structures display different intrinsic characteristics, resulting in significantly different influences on skin delivery. A concentration of 10% MX was determined to be the maximum loading capacity in the vesicle formulation. Thus, it was concluded that 0–40%mol Chol and surfactant and 10%mol MX-loaded vesicle formulations were desirable for further optimization to develop model vesicle

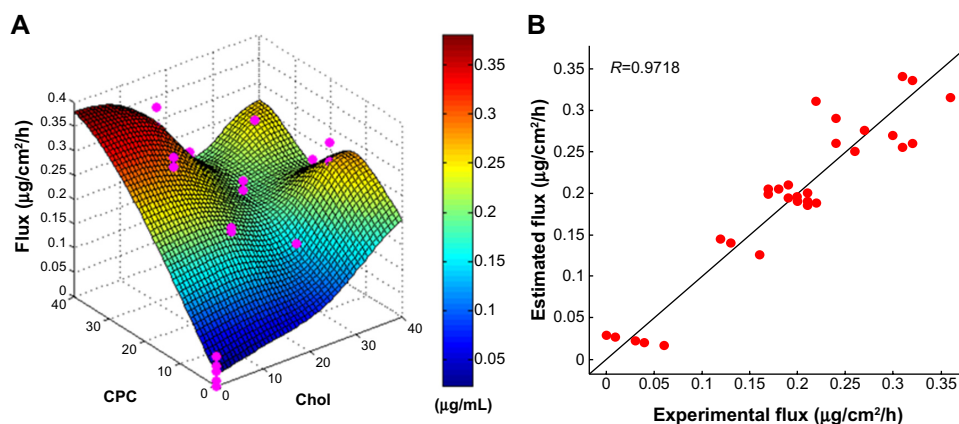


**Figure 2** The response surface for the skin permeation flux (A) and the reliability (B) of the model formulation.

**Abbreviations:** Chol, cholesterol; CPC, cetylpyridinium chloride; h, hour.

formulations. The 12 model formulations obtained from the two-factor spherical second-order composite experimental design were formulated and evaluated based on the original data set using RSM-S. A response surface and its reliability for the flux variable of the model formulation are illustrated in Figure 2. The search direction for the response variables was set to produce a high flux value. Moreover, to confirm the accuracy and reliability of the optimal formulation estimated using RSM-S, the optimal formulation was confirmed by experiment. It was found that the skin permeation flux value predicted by the RSM-S (predicted flux =  $0.31 \mu\text{g}/\text{cm}^2/\text{hour}$ ) was very close to the experimental value ( $0.31 \pm 0.6 \mu\text{g}/\text{cm}^2/\text{hour}$ ). This high reliability suggested that the vesicle composition

ratio of the optimal formulation (PC/Chol/surfactant/MX 0.77%:0.04%:0.10%:0.07% w/v ratio) could be used as the model formulation ratio in further experiments. Moreover, the morphology of the three-dimensional optimal model formulation was further observed using freeze-fractured transmission electron microscopy to determine the details of the vesicular morphology. Nano-sized, smooth surfaces and spherical vesicles were observed, as depicted in Figure 3.

### Effect of surfactant charge

The physicochemical characteristics of the A-TFS, N-CLP, and C-TFS outlined in Table 2 reveal that the addition of anionic surfactant, ie, SHS in A-TFS, and cationic surfactant, ie, CPC in C-TFS, produced significant differences in vesicle size (nm), zeta potential (mV), elasticity ( $\text{mg} \cdot \text{sec}^{-1} \cdot \text{cm}^{-2}$ ) and EE (%) compared with N-CLP. A-TFS displayed a large vesicle size ( $\sim 164 \text{ nm}$ ) with a negative charge ( $\sim -60.8 \text{ mV}$ ). In contrast, C-TFS exhibited a small vesicle size ( $\sim 90 \text{ nm}$ ) with a positive charge ( $\sim +48.3 \text{ mV}$ ). Moreover, the elasticity and EE of both types of transfersome (A-TFS and C-TFS) were higher than that of N-CLP. The neutralization of the anionic drug (MX) and cationic vesicles (C-TFS) may have resulted in smaller vesicle sizes due to a reduction in the repulsive forces in the C-TFS bilayer. In contrast, the synergistic effects of the anionic drug (MX) and anionic vesicles (A-TFS) may have resulted in large vesicle sizes due to the induction of repulsive forces in the A-TFS bilayer.<sup>13</sup> The vesicle formulations were composed of neutral material, ie, Chol, and positively and negatively charged surfactants, ie, CPC and SHS, respectively. Under the experimental condition of pH 5.5, the isoelectric point (PI) of PC (PI = 6) was higher than the pH. However, the PI of MX (PI = 2.6) was lower than the pH. Therefore, PC and MX displayed a net positive charge and a net negative charge, respectively. Thus,

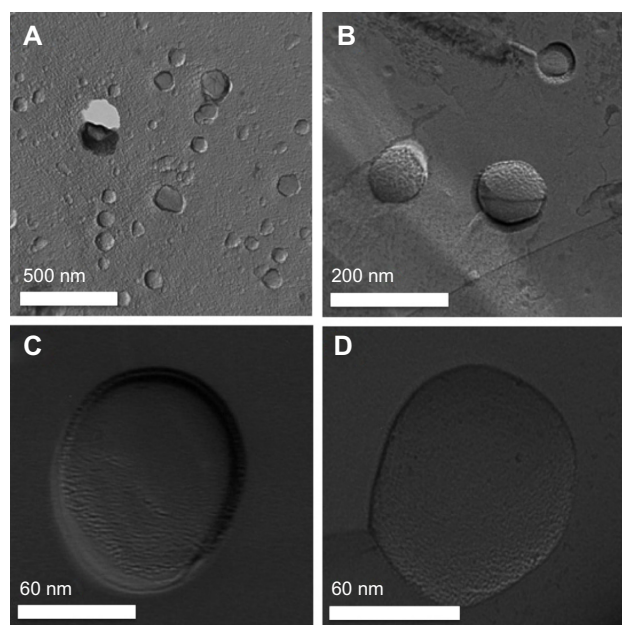


**Figure 3** Freeze-fractured transmission electron microscopy images of the optimized meloxicam-loaded vesicle formulation.

**Notes:** (A) 5,000 $\times$ ; (B) 30,000 $\times$ ; (C) 100,000 $\times$ ; (D) 100,000 $\times$ .

**Table 2** Effect of the surfactant on vesicle size, zeta potential, elasticity and entrapment efficiency of the vesicle formulation (mean  $\pm$  standard error)

	Vesicle size (nm)	Zeta potential (mV)	Elasticity (mg · sec <sup>-1</sup> · cm <sup>-2</sup> )	Entrapment efficiency (%)
Effect of surfactant charge				
A-TFS	164.3 $\pm$ 3.2	-60.8 $\pm$ 0.51	19.2 $\pm$ 1.68	54.11 $\pm$ 0.33
N-CLP	108.8 $\pm$ 10.6	1.3 $\pm$ 1.01	11.6 $\pm$ 1.64	26.36 $\pm$ 0.26
C-TFS	90.6 $\pm$ 9.2	48.3 $\pm$ 0.67	88.7 $\pm$ 0.98	68.06 $\pm$ 0.84
Effect of surfactant carbon chain length				
C4	113.3 $\pm$ 3.5	10.9 $\pm$ 3.21	120.1 $\pm$ 2.87	9.92 $\pm$ 0.41
C12	94.5 $\pm$ 2.0	26.9 $\pm$ 2.63	108.7 $\pm$ 1.74	46.11 $\pm$ 0.29
C16	90.6 $\pm$ 9.2	48.3 $\pm$ 0.67	88.7 $\pm$ 0.98	68.06 $\pm$ 0.84
Effect of surfactant content				
0% CPC	108.8 $\pm$ 10.6	1.3 $\pm$ 1.01	11.6 $\pm$ 1.64	26.36 $\pm$ 0.26
10% CPC	78.8 $\pm$ 9.2	36.6 $\pm$ 1.37	23.6 $\pm$ 2.40	29.51 $\pm$ 0.98
20% CPC	81.6 $\pm$ 1.0	39.7 $\pm$ 3.98	52.6 $\pm$ 1.32	47.25 $\pm$ 0.67
29% CPC	90.6 $\pm$ 9.2	48.3 $\pm$ 0.67	88.7 $\pm$ 0.98	68.06 $\pm$ 0.84

**Abbreviations:** A-TFS, anionic transfersomes; CPC, cetylpyridinium chloride; C-TFS, cationic transfersomes; N-CLP, neutral conventional liposomes.

the net charges of A-TFS, N-CLP, and C-TFS were negative, neutral, and positive, respectively, as a result of the intrinsic properties of their surfactants and the total net charge of the liposome composition. SHS and CPC exhibit a high radius of curvature, which can destabilize and increase the deformability of the vesicle bilayer, thus increasing its fluidity or elasticity.<sup>22</sup> The carbon chain lengths of CPC and SHS were the same, but C-TFS exhibited a stronger interaction with the bilayer than SHS due to its significantly higher elasticity. This result suggests that the hydrophilic head group of the surfactant directly affects the elasticity of the vesicle bilayer. The beneficial roles of SHS and CPC within transfersomes were readily apparent, as the intrinsic properties of the surfactants led to the increased solubility of MX in the vesicle bilayer and therefore EE values for A-TFS and C-TFS that were significantly higher than that of N-CLP. Our results were consistent with a previous study that demonstrated that the EE of a drug in phosphatidylethanolamine vesicles is significantly increased when sodium stearate (anionic surfactant) is incorporated into the vesicles.<sup>23</sup>

### Effect of surfactant carbon chain length

The physicochemical characteristics of MX-loaded vesicle formulations containing short-chain (butylpyridinium chloride [C4]), medium-chain (laurylpyridinium chloride [C12]) and long-chain (cetylpyridinium chloride [C16]) carbons are shown in Table 2. The vesicle size and elasticity decreased slightly with increasing carbon chain length in the order of C4, C12, and C16. The vesicle size and elasticity decreased approximately 20% and 26%, respectively, as C4 was substituted by C16. Surfactants with longer carbon chains may increase vesicle rigidity by

inserting deeper into the bilayer; thus, increasing the carbon chain length led to decreased vesicle size. Meanwhile, the vesicle size and zeta potential of liposomes containing 1,2-dimyristoyl-sn-glycero-3-phosphocholine ([DMPC] C14), 1,2-dipalmitoyl-sn-glycero-3-phosphocholine (C16), and 1,2-distearoyl-sn-glycero-3-phosphocholine ([DSPC] C18) and loaded with midazolam or propofol were not significantly influenced by the lipids having the same head group.<sup>24</sup> The insertion of C8 (short-chain carbon) resulted in decreased vesicle sizes in the order of poly(asparagines) grafted with C8, C12, C18, and C22.<sup>25</sup> These results suggest that varying trends in vesicle size may be influenced by the hydrophilic head group of the surfactant and the method of preparation. The zeta potential increased significantly with increasing carbon chain length in the order of C4, C12, and C16, with an increase of approximately 77% when C4 was substituted with C16. These results could be due to the intrinsic properties of each surfactant. The hydrophobicity of long-chain carbons is greater than that of short-chain carbons, and long-chain carbons could have led to increased solubility of the surfactant molecule in the PC bilayer. The amount of long-chain carbons in the PC bilayer was greater than the amount of short-chain carbons, and long-chain carbons might therefore exhibit stronger electrostatic interactions and zeta potentials than short-chain carbons. The elasticity of the vesicle increased in the order of C16, C12, and C4. These results are consistent with the findings of Park et al, in which the elasticity was observed to increase with decreasing carbon chain length (increased in the order of C22, C18, C12, and C8).<sup>25</sup> Because long-chain carbons exhibit strong hydrophobic interactions with PC, the PC bilayer of the vesicles becomes tighter. Long-chain carbons decrease the

elasticity of the vesicle through their deep insertion into the PC bilayer. Furthermore, short-chain carbons increase the elasticity of the vesicle through their shallow insertion into the PC bilayer. Therefore, the EE significantly increased with increasing carbon chain length in the order of C4, C12, and C16, with an ~85% increase when C4 was substituted with C16. These results are consistent with Ali et al, who demonstrated that an increase in carbon chain length led to an increase in the encapsulation of hydrophobic drugs, such as propofol and midazolam, into vesicles.<sup>24</sup> Increasing the carbon chain length was also found to increase the encapsulation of water-insoluble drugs, such as ibuprofen, into vesicles in the order of DMPC (C14); DSPC (C18); and dilignoceryl PC (C24).<sup>10</sup> The increase in the EE values of long-chain carbons could be attributed to the increased hydrophobic area within the PC bilayer.<sup>10,26</sup>

### Effect of surfactant content

The physicochemical characteristics of MX-loaded vesicles composed of varying contents of surfactant, including the control (0% CPC) and low (10% CPC), medium (20% CPC), and high (29% CPC) surfactant contents, are shown in Table 2. The vesicle size and zeta potential tended to increase slightly, while the elasticity and EE significantly increased in the order of 10% CPC, 20% CPC, and 29% CPC. The vesicle size, zeta potential, elasticity, and EE increased by approximately 13%, 23%, 73%, and 56%, respectively, when 10% CPC was substituted with 29% CPC. The trends in increasing vesicle size, zeta potential, elasticity, and EE were recognized as intrinsic properties of the surfactant. Liu et al demonstrated that an increase in the biosurfactant produced by some *Bacillus subtilis* strains from 0.05–0.24 mg/mL resulted in a decrease in the vesicle size of soy PC liposomes.<sup>27</sup> However, Mohammed et al demonstrated that an increase in stearylamine (cationic surfactant) from 1–6  $\mu$ M resulted in an increase in the vesicle size of egg PC liposome.<sup>10</sup> The insertion of surfactant into the vesicle bilayer can increase its curvature and result in decreased vesicle size.<sup>25</sup> However, the net effect on vesicle size in the present study was influenced by other factors. In addition to the method of preparation, the drug loading in the vesicle bilayer may result in increased vesicle size, as confirmed by the study of Mohammed et al.<sup>10</sup>

### In vitro skin permeation

Figure 4 shows the graphic plot of the cumulative skin permeation per unit area and the steady-state flux of various MX-loaded vesicle formulations over an incubation period

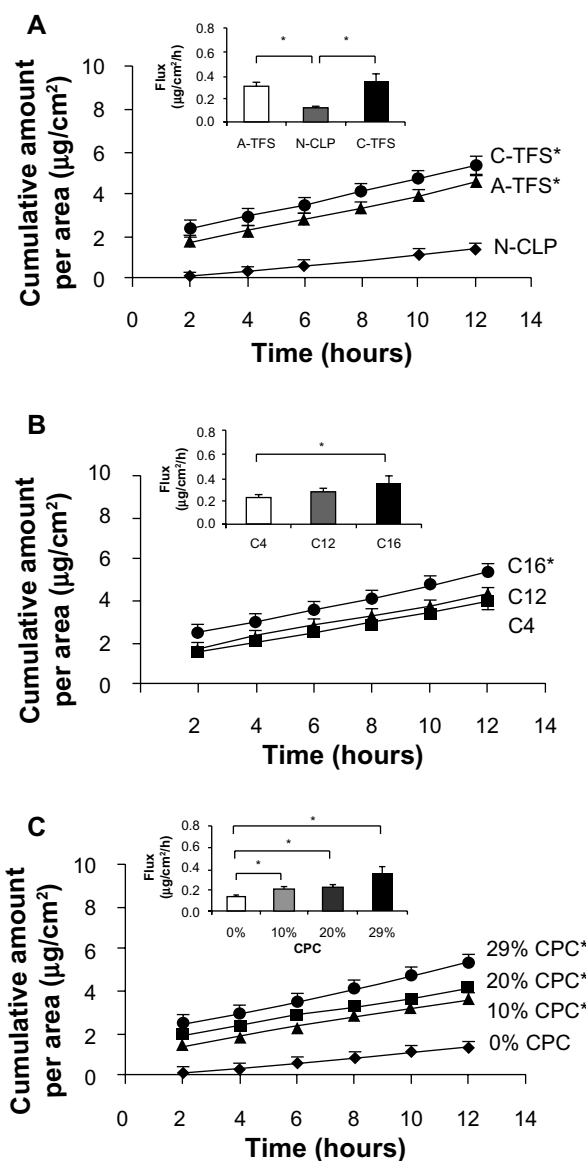


**Figure 4** The influence of (A) surfactant charge, (B) surfactant carbon chain length, and (C) surfactant content on the skin permeation profile and the steady-state flux of the vesicle formulation (n=3). \*is statistical significance (P-value <0.05). **Abbreviations:** A-TFS, anionic transfersomes; CPC, cetylpyridinium chloride; C-TFS, cationic transfersomes; h, hour; N-CLP, neutral conventional liposomes.

of 2–12 hours. The skin permeabilities (skin permeation profile and steady-state flux) of A-TFS and C-TFS were not significantly different, while the skin permeabilities of the charged transfersomes were significantly greater than those of the non-charged liposomes (N-CLP). The steady state flux of A-TFS and C-TFS were significantly higher than N-CLP, at approximately 58% and 63%, respectively. The surfactants SHS and CPC in A-TFS and C-TFS can open the dense keratin structures in corneocytes, and both anionic and cationic surfactants swell the SC and interact with the intercellular keratin, thus increasing the skin permeation of various drugs (eg, hydrocortisone, lidocaine).<sup>28</sup> Surfactants can interact with



skin constituents in many ways. For example, surfactants are widely known to interact with proteins, and thus can inactivate enzymes and bind strongly within the SC. They can swell the SC (most likely by uncoiling the keratin fiber and altering the  $\alpha$ -helices to a  $\beta$ -sheet conformation) and are able to modify the binding of water to the SC. Anionic surfactant-treated SC is somewhat brittle, possibly due to the extraction of natural moisturizing factor. Cationic surfactants are also able to extract lipids from the SC and can disrupt the lipid bilayer packing within the tissue.<sup>29</sup> Clearly, cationic surfactants cause a greater increase in the steady-state flux of MX than anionic surfactants, which, in turn, cause a greater increase in the flux than N-CLP. Ashton et al<sup>30</sup> compared the effects of dodecyltrimethylammonium bromide (as cationic surfactant), sodium lauryl sulfate (as anionic surfactant), and dodecoxyethanol (Brij 36T) (as non-ionic surfactant) on the *in vitro* flux of methyl nicotinamide across excised human skin and reported that permeation enhancement occurred in the following order: cationic, anionic, neutral. However, Brij 36T was shown to exert a small effect on the permeability but a more immediate effect on skin permeation.<sup>28</sup> This result revealed that the anionic and/or cationic surfactants significantly affected the skin permeation of MX across the skin by swelling the SC and interacting with intercellular keratin. However, the crossing of transfersomes across the skin was attributed to the high deformability of these specialized vesicles due to the accumulation of these single-chain surfactants at sites of high stress as a result of their increased propensity to form high-curvature structures. This rearrangement was claimed to reduce the energy required for deformation; the stress was reportedly produced upon drying of the vesicles, which, being flexible, were able to follow the transdermal hydration gradient.<sup>7</sup>

In our study, the skin permeability of the transfersomes increased when the carbon chain length of the surfactant increased. The skin permeability of the vesicle formulation increased with increasing chain length in the order C4, C12, and C16. The skin permeability of C16 was significantly greater than C4, with an approximately 17% increase when C4 was substituted with C16. These results are consistent with a previous study,<sup>31</sup> which demonstrated that, as the carbon chain length in the vesicle increased from C7 to C12, the permeation of naloxone increased. Ogiso and Shintani revealed that C12–C14 were the most effective carbon chain lengths used in increasing the permeation of propranolol.<sup>32</sup> Duangjit et al reported that C18–C24 were more effective than C32 in the permeation of MX.<sup>18</sup> Short-chain carbons may suffer from insufficient lipophilicity for

skin permeation, whereas longer-chain fatty acids might have much higher affinities for lipids in the SC, thereby hindering their permeation. Our study suggests that C16 possesses an optimal balance between partition coefficient and affinity to the skin. The results revealed that skin permeability is also affected by the carbon chain length of the surfactant.

The surfactant content affected skin permeability, with the skin permeability of the transfersomes increasing with increasing surfactant content. The skin permeability of the vesicle formulation increased in the order 0% CPC, 10% CPC, 20% CPC, and 29% CPC. The skin permeabilities of the 29% CPC, 20% CPC, and 10% CPC formulations were significantly higher than that of 0% CPC, by approximately 63%, 41%, and 35%, respectively. This result reveals that the surfactant content significantly affected the skin permeability of the vesicle formulation due to the intrinsic properties of the surfactant (CPC), as reported above.

The present studies demonstrated that the surfactant factor (ie, charge, carbon chain length, and content of surfactant) directly affected the skin permeability of MX.

## Stability evaluation

The physicochemical stabilities of MX-loaded vesicle formulations from day 1 to day 120 at 4°C and 25°C were evaluated for recommended storage conditions. After storage at 4°C for 30 days, the MX content had slightly decreased but remained at 90% of the initial formulation. After storage at 25°C for 30 days, the MX remaining in nearly all of the formulations had decreased slightly but remained at 90% and 80% of the initial formulation at day 15 and day 30, respectively. However, after storage at 4°C and 25°C for 120 days, the MX remaining in nearly all of the formulations had decreased by approximately 70%–80% and 80%–90% from the initial formulation, respectively (Figure 5). The physicochemical stabilities (ie, vesicle size and zeta potential) of the vesicle formulations were not significantly different between the experimental temperatures of 4°C and 25°C over a period of 30 days. The physicochemical stabilities of nearly all of the vesicle formulations exhibited similar trends to the MX-remaining results, indicating the good physicochemical stability of our vesicle formulations at 4°C for 30 days as well as at 25°C for 15 days. In our study, the addition of Chol was essential to the vesicle formulation, which can be attributed to Chol's stabilizing effects.<sup>33,34</sup> The physicochemical stability of the vesicle formulation was not significantly different between the experimental temperatures of 4°C and 25°C over 30 days, while the physicochemical stability of the vesicle formulation at the two experimental temperatures (ie, 4°C and 25°C) was significantly different between day 1 and

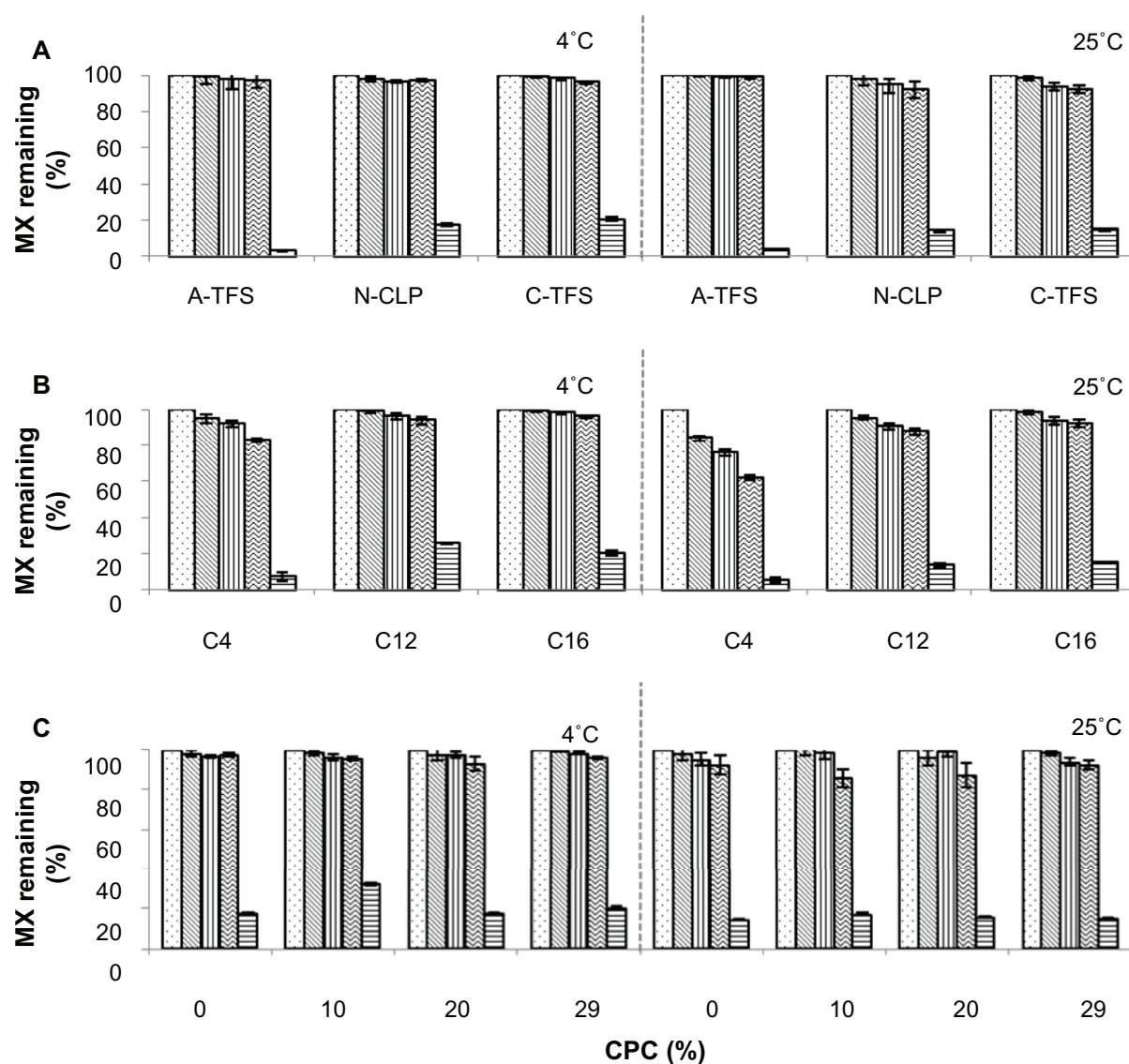


**Figure 5** The influence of (A) surfactant charge, (B) surfactant carbon chain length, and (C) surfactant content on the remaining MX at different days (n=3).

**Notes:** □ Day 1; ▨ day 7; ▩ day 15; ▪ day 30; ▫ day 120.

**Abbreviations:** A-TFS, anionic transfersomes; C-TFS, cationic transfersomes; MX, meloxicam; N-CLP, neutral conventional liposomes; CPC, cetylpyridinium chloride.

day 120 of storage. Therefore, the storage duration was the primary factor affecting the physicochemical stability of the vesicle formulation in this study. The recommended storage conditions for the vesicle formulation are therefore 4°C for 30 days and/or 25°C for 15 days.

## The mechanisms of liposomes on skin permeation

Changes in the ultra-structures of the intercellular lipids occurred following the treatment of skin with the vesicle formulation, as shown in the FTIR spectra and DSC thermograms (Figure 6). The FTIR peaks from the absorption-broadened C–H ( $\text{CH}_2$ ) symmetric and asymmetric stretches are near  $2,850\text{ cm}^{-1}$  and  $2,920\text{ cm}^{-1}$ , respectively. These

peaks in the FTIR spectra of the skin treated with the vesicle formulation shifted from  $2,850\text{ cm}^{-1}$  to  $2,850.7\text{--}2,851.3\text{ cm}^{-1}$  and from  $2,920\text{ cm}^{-1}$  to  $2,920.3\text{--}2,920.9\text{ cm}^{-1}$ , respectively. Meanwhile, the DSC thermograms also displayed peak shifts, from  $231.72^\circ\text{C}$  for the skin sample treated with the MX suspension (control) to a lower transition temperature for the skin sample treated with the vesicle formulations. The SC lipid of the skin sample existed in the liquid state. The shifted peak of the skin samples were in range of  $229.18^\circ\text{C}\text{--}230.53^\circ\text{C}$ , depending on vesicle formulation. These results are consistent with previous studies,<sup>35–38</sup> which demonstrated that liposome vesicles do not penetrate into the SC but rather that the lipid components of the vesicles can penetrate and change the enthalpy of the SC lipid-related

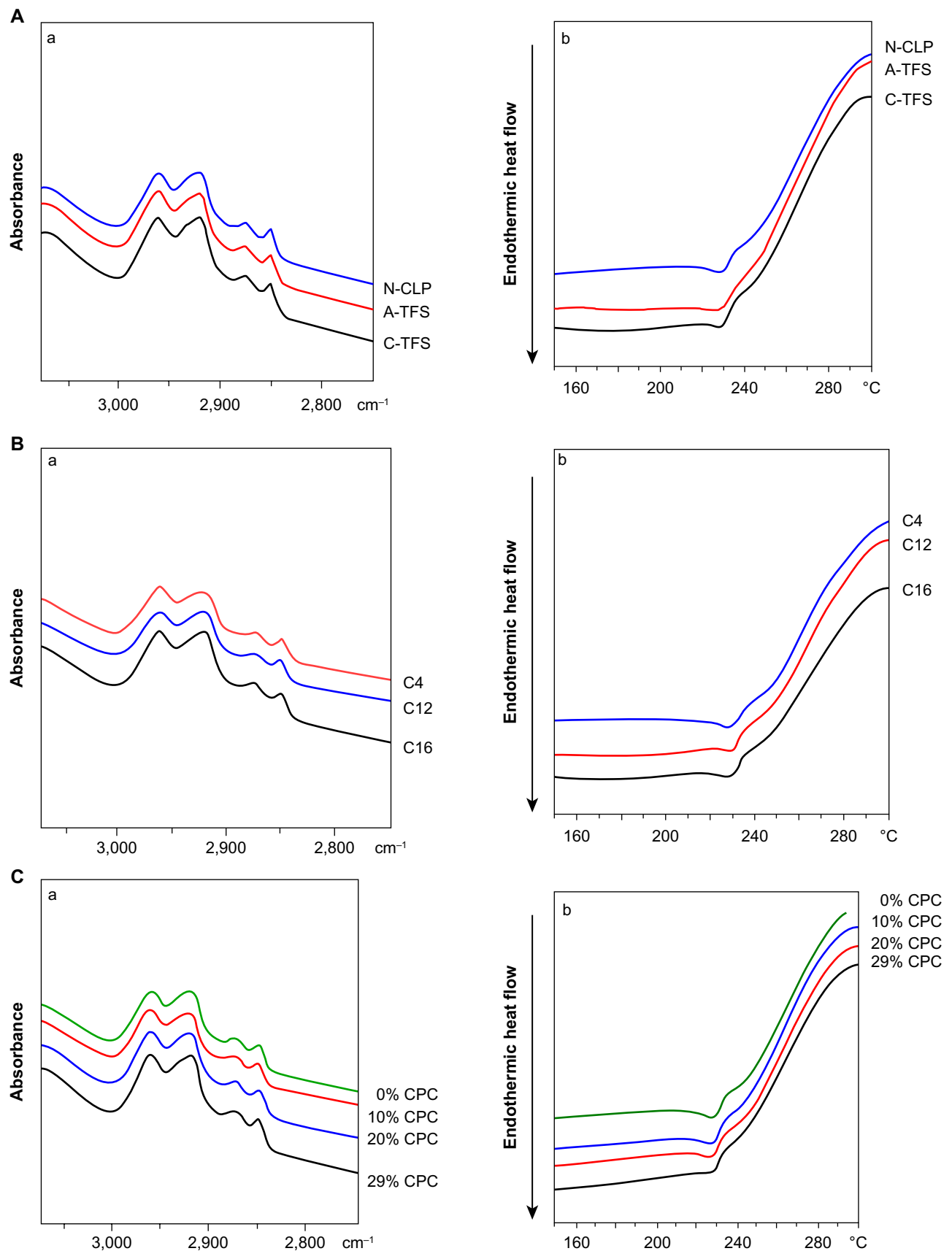


**Figure 6** The influence of (A) surfactant charge, (B) surfactant carbon chain length, and (C) surfactant content of the shed snake skin after skin permeation. **Notes:** (a) Fourier transform infrared spectra; (b) differential scanning calorimetry thermograms.

**Abbreviations:** A-TFS, anionic transfersomes; CPC, cetylpyridinium chloride; C-TFS, cationic transfersomes; N-CLP, neutral conventional liposomes.

transitions of the skin. The present study suggested that the SC lipid arrangement of the skin sample treated with the vesicle formulation was disrupted by altering the fluidity or flexibility of the SC lipids. The interruption of the SC lipids by vesicle formulation or by the vesicle components caused an increase in the skin permeability of MX; the FTIR spectra and DSC thermograms also support the conclusions of this in vitro skin permeation study.

The vesicles may adsorb to the SC surface with subsequent transfer of the drug directly from the vesicles to the skin, or the vesicles may fuse and mix with the SC lipid matrix, increasing drug partitioning into the skin. Our results indicate that the vesicles can be taken into the skin but cannot penetrate through the intact, healthy SC; instead, they dissolve and form a unit membrane structure with the skin sample, as evidenced by the alteration and rearrangement of the lipid structures of the skin sample treated with the vesicles, as revealed by FTIR and DSC characterization (Figure 6).

## Conclusion

In this study, surfactant charge, surfactant carbon chain length, and surfactant content directly affected the physicochemical characteristics of vesicles and their skin permeability. The incorporation of a high content (29%) of cationic surfactant (CPC) with a long-chain carbon (C16) into the vesicle formulation improved the skin permeability of MX. The optimal formulation comprised PC/Chol/CPC/MX in a 0.77%:0.04%:0.10%:0.07% w/v ratio and is recommended as the optimal liposome for the skin delivery of MX. The possible mechanisms by which these liposomes improved the skin delivery of MX encompassed the penetration-enhancing mechanism and the vesicle adsorption to and/or fusion with the SC. Our findings provide useful fundamental information for the development and design of novel liposome formulations for enhancing the TDD of lipophilic drugs.

## Acknowledgments

The authors are grateful to the Thailand Research Funds through the Royal Golden Jubilee PhD Program (grant number PHD/0141/2552), and the Basic Research Grant (grant number BRG 5680016), Faculty of Pharmacy, Silpakorn University, Thailand and Department of Pharmaceutics, Hoshi University, Japan for facilities and support. The authors gratefully acknowledge Professor Yoshie Maitani and Dr Kumi Kawano of the Department of Drug Delivery Research, Hoshi University for their helpful assistance with determination of liposome elasticity, and also Professor Satoru Kato and Tsubasa Miyoshi for their helpful assistance of liposomes characterization using freeze-fractured

transmission electron microscopy at the Department of Physics, Kwansai Gakuin University, Hyogo, Japan. Finally, the authors would like to acknowledge Assistant Professor Dr Warisada Sila-on of the Faculty of Pharmaceutical Sciences, Ubon Ratchathani University, Ubon Ratchathani, Thailand for facilities and support.

## Disclosure

The authors report no conflicts of interest in this work.

## References

- Engelhardt G, Homma D, Schlegel K, Utzmann R, Schnitzer C. Anti-inflammatory, analgesic, antipyretic and related properties of meloxicam, a new non-steroidal anti-inflammatory agent with favourable gastrointestinal tolerance. *Inflamm Res*. 1995;44:423–433.
- Luger P, Daneck K, Engel W, Trummlitz G, Wagner K. Structure and physicochemical properties of meloxicam, a new NSAID. *Eur J Pharm Sci*. 1996;4:175–187.
- Degner F, Sigmund R, Zeidler H. Efficacy and tolerability of meloxicam in an observational, controlled cohort study in patients with rheumatic disease. *Clin Ther*. 2000;22:400–410.
- Bjarnason I, Hayllar J, MacPherson AJ, Russell AS. Side effects of nonsteroidal anti-inflammatory drugs on the small and large intestine in humans. *Gastroenterology*. 1993;104(6):1832–1847.
- Yuan Y, Li SM, Mo FK, Zhong DF. Investigation of microemulsion system for transdermal delivery of meloxicam. *Int J Pharm*. 2006;321:117–123.
- Jantharaprapap R, Stagni G. Effects of penetration enhancers on in vitro permeability of meloxicam gels. *Int J Pharm*. 2007;343:26–33.
- Cevc G, Schätzlein A, Blume G. Transdermal drug carriers: basic properties, optimization and transfer efficiency in the case of epicutaneously applied peptides. *J Control Release*. 1995;36:3–16.
- Montenegro L, Panico AM, Ventimiglia A, Bonina FP. In vitro retinoic acid release and skin permeation from different liposome formulations. *Int J Pharm*. 1996;133:89–96.
- Katahira N, Murakami T, Kugai S, Yata N, Takano M. Enhancement of topical delivery of a lipophilic drug from charged multilamellar liposomes. *J Drug Target*. 1999;6:405–414.
- Mohammed AR, Weston N, Coombes AG, Fitzgerald M, Perrie Y. Liposome formulation of poorly water soluble drugs: optimisation of drug loading and ESEM analysis of stability. *Int J Pharm*. 2004;285:23–34.
- Song YK, Kim CK. Topical delivery of low-molecular-weight heparin with surface-charged flexible liposomes. *Biomaterials*. 2006;27(2):271–280.
- Sinico C, Manconi M, Peppi M, Lai F, Valenti D, Fadda AM. Liposomes as carriers for dermal delivery of tretinoin: in vitro evaluation of drug permeation and vesicle-skin interaction. *J Control Release*. 2005;103:123–136.
- Manosroi A, Khanrin P, Lohcharoenkai W, et al. Transdermal absorption enhancement through rat skin of gallidermin loaded in niosomes. *Int J Pharm*. 2010;392:304–310.
- Gillet A, Compère P, Lecomte F, et al. Liposome surface charge influence on skin penetration behaviour. *Int J Pharm*. 2011;411:223–231.
- Takayama K, Nagai T. Simultaneous optimization for several characteristics concerning percutaneous absorption and skin damage of keto-profen hydrogels containing d-limonene. *Int J Pharm*. 1991;74(2–3):115–126.
- Ueda N, Nakano R. Estimating expected error rates of neural network classifiers in small sample size situations: a comparison of cross-validation and bootstrap. *IEEE International Conference Neural Networks Proceeding*; 27 Nov 1995–01 Dec 1995, 1995; Perth, WA.
- Dupret G, Koda M. Bootstrap resampling for unbalanced data in supervised learning. *Eur J Oper Res*. 2001;134:141–156.

18. Duangjit S, Opanasopit P, Rojanarata T, Ngawhirunpat T. Characterization and in vitro skin permeation of meloxicam-loaded liposomes versus transfersomes. *J Drug Deliv*. 2011;2011:418316.
19. Shotton DM, Servers NJ. An introduction to freeze fracture and deep etching. In: Servers NJ, Shotton DM, editors. Rapid freezing, freeze fracture, and deep etching. New York: Wiley-Liss; 1995:1–31.
20. Cevc G. Material Transport Across Permeability Barriers by Means of Lipid Vesicles. In: Lipowsky R, Sackmann E, editors. Handbook of Biological Physics. Amsterdam: Elsevier; 1995:465–490.
21. Ngawhirunpat T, Panomsuk S, Opanasopit P, Rojanarata T, Hatanaka T. Comparison of the percutaneous absorption of hydrophilic and lipophilic compounds in shed snake skin and human skin. *Pharmazie*. 2006;61:331–336.
22. Elsayed MM, Abdallah OY, Naggat VF, Khalafallah NM. Lipid vesicles for skin delivery of drugs: reviewing three decades of research. *Int J Pharm*. 2007;332:1–16.
23. Fang YP, Tsai YH, Wu PC, Huang YB. Comparison of 5-aminolevulinic acid-encapsulated liposome versus ethosome for skin delivery for photodynamic therapy. *Int J Pharm*. 2008(356):144–152.
24. Ali MH, Moghaddam B, Kirby DJ, Mohammed AR, Perrie Y. The role of lipid geometry in designing liposomes for the solubilisation of poorly water soluble drugs. *Int J Pharm*. 2013;453(1):225–232.
25. Park SI, Lee EO, Kim JW, Kim YJ, Han SH, Kim JD. Polymer-hybridized liposomes anchored with alkyl grafted poly(asparagine). *J Colloid Interface Sci*. 2011;364:31–38.
26. Dan N. Lipid tail chain asymmetry and the strength of membrane-induced interactions between membrane proteins. *Biochim Biophys Acta*. 2007;1768:2393–2399.
27. Liu J, Zou A, Mu B. Surfactin effect on the physicochemical property of PC liposome. *Colloids Surf A Physicochem Eng Asp*. 2010;361:90–95.
28. Barry BW. Penetration enhancer classification. In: Smith, Maibach HI, editors. *Percutaneous Penetration Enhancers*. 2nd ed. Boca Raton, FL: CRC Press; 2006:3–15.
29. Williams AC. *Transdermal and Topical Drug Delivery: From Theory to Clinical Practice*. London: Pharmaceutical Press; 2003.
30. Ashton P, Walters KA, Brain KR, Hadgraft J. Surfactant effects in percutaneous absorption. I. Effects on the transdermal flux of methyl nicotinate. *Int J Pharm*. 1992;87:261.
31. Aungst BJ, Rogers NJ, Shefter E. Enhancement of naloxone penetration through human skin in vitro using fatty acids, fatty alcohols, surfactants, sulfoxides and amides. *Int J Pharm*. 1986;33:225–234.
32. Ogiso T, Shintani M. Mechanism for the enhancement effect of fatty acids on the percutaneous absorption of propranolol. *J Pharm Sci*. 1990;79:1065.
33. Liu D, Chen W, Tsai L, Yang S. Microcalorimetric and shear studies on the effects of cholesterol on the physical stability of lipid vesicles. *Colloids Surf A Physicochem Eng Asp*. 2000;172:57–67.
34. Nasserri B. Effect of cholesterol and temperature on the elastic properties of niosomal membranes. *Int J Pharm*. 2005;300:95–101.
35. Kato A, Ishibashi Y, Miyake Y. Effect of egg yolk lecithin on transdermal delivery of bunazosin hydrochloride. *J Pharm Pharmacol*. 1987;39:399–400.
36. Zellmer S, Pfeil W, Lasch J. Interaction of phosphatidylcholine liposomes with the human stratum corneum. *Biochim Biophys Acta*. 1995;1237:176–182.
37. Kirjavainen M, Urtili A, Jääskeläinen I, et al. Interaction of liposomes with human skin in vitro – the influence of lipid composition and structure. *Biochim Biophys Acta*. 1996;1304:179–189.
38. Obata Y, Utsumi S, Watanabe H, et al. Infrared spectroscopic study of lipid interaction in stratum corneum treated with transdermal absorption enhancers. *Int J Pharm*. 2010;389:18–23.

## International Journal of Nanomedicine

### Publish your work in this journal

The International Journal of Nanomedicine is an international, peer-reviewed journal focusing on the application of nanotechnology in diagnostics, therapeutics, and drug delivery systems throughout the biomedical field. This journal is indexed on PubMed Central, MedLine, CAS, SciSearch®, Current Contents®/Clinical Medicine,

Submit your manuscript here: <http://www.dovepress.com/international-journal-of-nanomedicine-journal>

Dovepress

Journal Citation Reports/Science Edition, EMBase, Scopus and the Elsevier Bibliographic databases. The manuscript management system is completely online and includes a very quick and fair peer-review system, which is all easy to use. Visit <http://www.dovepress.com/testimonials.php> to read real quotes from published authors.